

Optimal Object Placement using a Virtual Axis

Martin Weiß

Ostbayerische Technische Hochschule Regensburg
Faculty of Computer Science and Mathematics
Regensburg, Germany
`martin.weiss@oth-regensburg.de`

Abstract. A basic task in the design of a robotic production cell is the relative placement of robot and workpiece. The fundamental requirement is that the robot can reach all process positions; only then one can think further optimization. Therefore an algorithm that automatically places an object into the workspace is very desirable. However many iterative optimization algorithms cannot guarantee that all intermediate steps are reachable, resulting in complicated procedures. We present a novel approach which extends a robot by a virtual prismatic joint - which measures the distance to the workspace - such that any TCP frames are reachable. This allows higher order nonlinear programming algorithms to be used for placement of an object alone as well as the optimal placement under some differentiable criterion.

Keywords: optimization, virtual joint, inverse kinematics, nonsmooth optimization, workspace, Cartesian tasks

1 Problem Statement

We consider the following task: A robot should unload a storage box with a chess-board like structure containing $B_x \times B_y$ identical workpieces at positions P_{kl} , $k = 1, \dots, B_x$, $l = 1, \dots, B_y$, counted in the coordinate directions of the frame $C \in \mathbb{F}$ (where \mathbb{F} denotes the set of all frames $\mathbb{R}^3 \times \text{SO}(3)$) associated with the box at distances D_x and D_y . Think of test-tubes in medicine or small parts in general production. The cell setup is considered fixed, so only the placement of the box in the cell can be chosen, e.g. because a new order type.

Usually a pick-and-place operation is programmed at one corner only, the other position commands are computed from this corner position and the indices and distances. However it is difficult for the user to assess whether all positions are reachable because of nonlinearity and axis limits. Testing the corners is a heuristic that works in many cases but there is no guarantee, so one has to run time-consuming tests. When the process needs to work on an object from different sides or with different orientations the situation is even more complicated. So the user would like to have an algorithm that determines a feasible object frame C near some initial guess C_0 , maybe additionally optimizing one of the many known manipulability measures, see [8], [12].

It is easy to check in a program whether a given frame C leads to reachable positions or not but it is difficult for a nonlinear optimizer to determine a direction that leads to a "more feasible" situation: Feasibility is a binary decision; the backward transformation will usually issue an error only, and abort.

Our idea is to introduce a virtual joint as a *slack variable* in terms of nonlinear programming (see [9]) into the optimization problem that measures the distance of a position from feasibility. This variable therefore has an intuitive geometric interpretation. We can also interpret the virtual axis as a homotopy variable similar to [4] which gives an "easy" solution for large values. Our slack variable is not generated by the standard procedure replacing an inequality constraint $g(x) \leq 0$ by the equality $g(x) + z = 0$, with the sign constraining $z \geq 0$.

Our approach has some similarity to the introduction of virtual axes for singularity avoidance in [10] or [7]. However we do not introduce a rotational joint to reduce velocities near singularities but rather use a prismatic joint to enlarge the mathematical workspace in the optimization process. In combination with a smoothing operation we can use standard optimization algorithms which require differentiability of order 1 like all algorithms based on gradient descent, or order 2 like Sequential Quadratic Programming (SQP), cf. [9]. Our approach is not related at all to voxelization of the workspace like in [11] and other algorithms aiming at collision free planning.

2 Virtual Axis Approach

For ease of exposition we choose a 6R robot resembling the well known Puma 560 but with more zeros in the parameters. We could extend all formulae to similar 6R real industrial robots. We use the DH convention

$$R_z(q_i) \cdot T_z(d_i) \cdot T_x(a_i) \cdot R_x(\alpha_i) =: R_z(q_i) \cdot B_i =: A_i(q_i)$$

to get the wrist centre point (WCP) and tool centre point (TCP)

$$\begin{aligned} \text{WCP}(q) &= A_1(q_1) \cdot A_2(q_2) \cdot A_3(q_3) \cdot A_4(q_4) \cdot A_5(q_5) \cdot A_6(q_6) \\ \text{TCP}(q) &= \text{WCP}(q) \cdot \text{TOOL} \end{aligned}$$

expressed relative to the world coordinate system chosen as the axis 1 coordinate system. Note that $a_6 = d_6 = 0$ in our case so the DH chain ends in the WCP as the essential point for the backward transform. Figure 1 shows the robot data and the reference position. We use $l_{23} = 315$, $l_{35} = 365$ and a tool with $T_z(t_z)$, $t_z = 100$, pointing in direction z_6 from the flange. Lengths are measured in [mm], angles in [rad]. Note that joint 3 is pointing upward for $q = 0$, so the stretched position corresponds to $q_3 = -\frac{\pi}{2}$. We assume joint limits $-\pi \leq q_{\min,i} \leq q_i \leq q_{\max,i} \leq \pi$, $i = 1, \dots, 6$. As usual, this type of robots has up to 8 discrete solutions of the backward transform for non-singular positions. We identify these 8 configurations with an integer $s \in \{0, \dots, 7\}$.

Infeasibility of the backward transform for a given frame F and configuration s may arise from two reasons with different severity: First, the WCP may be to

i	θ_i	d_i	a_i	α_i	type
1	q_1	0	0	$\frac{\pi}{2}$	R
2	q_2	0	l_{23}	0	R
3	q_3	0	0	$-\frac{\pi}{2}$	R
4	q_4	l_{35}	0	$\frac{\pi}{2}$	R
5	q_5	0	0	$-\frac{\pi}{2}$	R
6	q_6	0	0	0	R

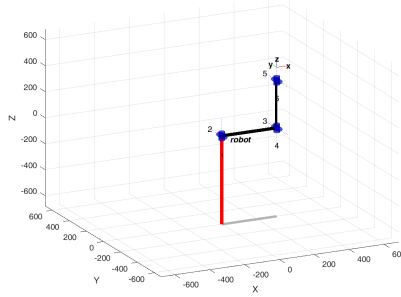


Fig. 1. DH parameters and reference position $q = 0$ for original robots

far from the robot such that the triangle construction for q_3 fails. There is no remedy in this case. Second, even if axis values q exist such that $\text{TCP}(q) = F$, these might violate the joint limits: $q_i \notin [a_i, b_i]$ for some i . This is no obstacle during the optimization process, only for a solution. So the second problem can be fixed by dropping the joint limits and allowing $q_i \in (-\pi, \pi]$, $i = 1, \dots, 6$. We describe this difference by a *physical* and a *mathematical* workspace \mathcal{W}_P and \mathcal{W}_M which are the WCP frames under the two joint restrictions under consideration:

$$\mathcal{W}_P = \text{WCP} \left(\prod_{i=1}^6 [q_{\min,i}, q_{\max,i}] \right), \quad \mathcal{W}_M = \text{WCP} ((-\pi, \pi]^6)$$

We have $\mathcal{W}_P \subseteq \mathcal{W}_M$ and $\mathcal{W}_P \neq \mathcal{W}_M$ in general but \mathcal{W}_M is still a bounded set, which is the first problem.

In order to use optimization algorithms which may leave the feasible set \mathcal{W}_M , our goal is to define a *virtual robot* which has a solution for the backward transform for any frame $F \in \mathbb{F}$ and any configuration s . So we associate to our *original robot* a *virtual robot* with an additional *virtual prismatic joint* between joints 3 and 4, which has no joint limits. Any WCP in \mathbb{R}^3 is reachable then. The variable of the virtual joint will be denoted v , the other joints keep their names giving a combined joint variable $\tilde{q} = (q_1, q_2, q_3, v, q_4, q_5, q_6) \in \mathbb{R}^7$. DH parameters of the virtual robot are shown in Figure 2.

Sufficient conditions for our approach are stated as two assumptions:

Assumption 1 - Reachability of \mathbb{R}^3 : The mapping of the original joints and the virtual joint to the WCP position is surjective onto \mathbb{R}^3 .

Assumption 2 - Reachability of $\text{SO}(3)$ Joints 4,5,6 form a central wrist parametrizing all of $\text{SO}(3)$, i.e. the mapping $(-\pi, \pi]^3 \rightarrow \text{SO}(3)$, $(q_4, q_5, q_6) \mapsto \text{R}_z(q_4) \cdot B_4 \cdot \text{R}_z(q_5) \cdot B_5 \cdot \text{R}_z(q_6)$ is surjective.

In our case Assumption 1 is satisfied because for any fixed q_3 value the virtual joint generates an infinite line with the WCP, the second joint rotates the line through a plane, the first joint rotates the plane through all \mathbb{R}^3 . Central wrists

i	θ_i	d_i	a_i	α_i	type
1	\tilde{q}_1	0	0	$\frac{\pi}{2}$	R
2	\tilde{q}_2	0	l_{23}	0	R
3	\tilde{q}_3	0	0	$-\frac{\pi}{2}$	R
4	0	v	0	0	P
5	\tilde{q}_4	l_{35}	0	$\frac{\pi}{2}$	R
6	\tilde{q}_5	0	0	$-\frac{\pi}{2}$	R
7	\tilde{q}_6	0	0	0	R

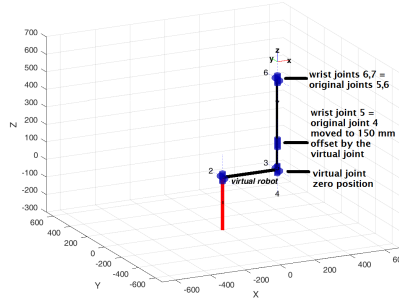


Fig. 2. DH parameters and reference position $\tilde{q} = (0, 0, 0, 150, 0, 0, 0)$ for virtual robot

satisfying Assumption 2 – for unbounded joint variables – are the most common choice in industry. Assumption 2 also guarantees an 8-solution kinematics. Using the notation WCP^v to distinguish the forward transform of the virtual robot we denote

$$\mathcal{W}_V = WCP^v \left((-\pi, \pi]^3 \times \mathbb{R} \times (-\pi, \pi]^3 \right).$$

Under our assumptions we get $\mathcal{W}_V = \mathbb{F}$. We call such a robot a *dextrous robot* because the dextrous workspace in \mathbb{R}^3 (points reachable with all orientations, see [2]) and reachable workspace (points reachable with at least one orientation) coincide, and are all of \mathbb{R}^3 .

3 Backward Transform with Redundancy Resolution

However we have introduced redundancy in our kinematics so we have to define a backward transform giving unique results. The virtual robot backward transform sets the virtual joint to the smallest absolute value such that a solution exists. In our case this is the distance between the WCP position and \mathcal{W}_M which is a hollow sphere for our robot so calculations are simple. Algorithm 1 uses the backward transform of the original robot: Note that both $l_{23} > l_{35}$ and $l_{23} < l_{35}$ lead to an empty interior, but $l_{23} < l_{35}$ results in negative v values. Also note that for our robot the stretched position for axis 3 is $q_3 = \pm \frac{\pi}{2}$, not 0 as in most industrial robots. This stretched position is used for all WCP positions outside \mathcal{W}_M .

For robots other than our simple one the computation of q_1 , as well as the definition of the stretched position and the computation of v have to be adapted.

4 Smoothness properties

The dexterity of the virtual robot makes all TCP frames feasible. Also the joint values \tilde{q} depend continuously on the TCP frame, if we keep the configuration fixed and avoid singularities or the original robot. Inside \mathcal{W}_M continuity is clear

Algorithm 1 virtual robot backward transform

Input: WCP frame F parametrized by $P = [x, y, z] \in \mathbb{R}^3$, $Q \in \text{SO}(3)$
Input: configuration coded as $s \in \{0, \dots, 7\}$
Output: virtual robot axes $\tilde{q} \in (-\pi, \pi]^3 \times \mathbb{R} \times (-\pi, \pi]^3$ with $\text{WCP}(\tilde{q}) = F$ where \tilde{q} corresponds to configuration s
if solution $q \in (-\pi, \pi]^6$ of original backward transform exists **then**
 return essentially this solution as $\tilde{q} = (q_1, q_2, q_3, 0, q_4, q_5, q_6)$
else
 compute q_1 using the original backward transform: $q_1 = \text{atan2}(y, x)$
 $d := \|P\|_2$, distance of WCP from robot base
 if P is outside of the hollow sphere, $d > l_{23} + l_{35}$ **then**
 $v := d - l_{23} - l_{35}$
 put joints 2 and 3 in stretched position $q_2 := \text{atan2}(z, r)$, $q_3 := -\frac{\pi}{2}$
 else
 P is in the empty interior of the hollow sphere, $d < |l_{23} - l_{35}|$
 $v := d - l_{23} + l_{35}$
 put joints 2 and 3 in stretched position $q_2 := \text{atan2}(z, r)$, $q_3 := +\frac{\pi}{2}$
 end if
end if

from the usual backward transformation formulae. When the WCP reaches the boundary of \mathcal{W}_M the triangles for the elbow-up and elbow-down configuration degenerate to a line and coincide, hence $q_3 \rightarrow -\frac{\pi}{2}$ which is the same value as when approaching from outside. Also $q_2 = \text{atan2}(z, r)$ depends continuously on the wrist centre point. However the dependence is not differentiable: When the wrist centre point enters \mathcal{W}_M from outside the solution for q_3 applies the cosine theorem to get $c = \cos(\varphi)$ near $\phi = \pi$. Computing $\varphi(c) = \text{atan2}(\pm\sqrt{1-c^2}, c)$ we get an infinite slope at $c = 1$, see Figure 3. This non-differentiability can affect all other axes.

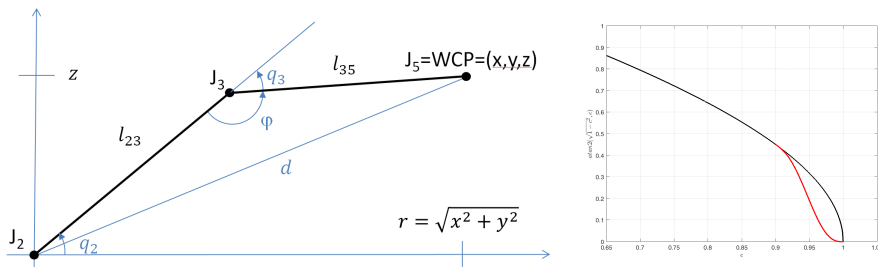


Fig. 3. Backward transform and smoothing

In order to get C^2 behaviour of all angles we modify $\varphi(c)$ on some interval $[1 - \epsilon, 1]$ with a polynomial of degree 5 with C^2 transition at $c = 1 - \epsilon$ and first and second derivative 0 at $c = 1$, see the red graph in Figure 3, right.

This is a basic idea in nonsmooth optimization [1]. Of course this distorts the backward transform and one has to check whether smoothing affects the optimal solution but the hope is that the optimum is sufficiently inside the workspace, and smoothing is only a temporary help for the optimization algorithm.

Figure 4 shows this behaviour for a motion of the virtual robot TCP from L_0 along the x axis to L_1 in height $z = 215$ with constant orientation Q with

$$L_0 = \begin{bmatrix} 500 \\ 0 \\ 215 \end{bmatrix}, \quad L_1 = \begin{bmatrix} 1300 \\ 0 \\ 215 \end{bmatrix}, \quad Q = \begin{bmatrix} -1 & 0 & 0 \\ 0 & 1 & 0 \\ 0 & 0 & -1 \end{bmatrix}$$

in the elbow-up configuration such that the tool is pointing downwards. The WCP crosses the boundary $\partial\mathcal{W}_M$ at

$$\partial x = \sqrt{(l_{23} + l_{35})^2 - (215 + t_z)^2} = \sqrt{680^2 - 315^2} \approx 602.6.$$

Axes q_1, q_4, q_6 do not move. All joints are continuous indeed with infinite slope of q_2, q_3, q_5 at ∂x . The left picture shows the axis values without smoothing, the right a zoom into the q_3 behaviour without and with smoothing. The virtual axis remains at $v = 0$ in \mathcal{W}_M , then v grows linearly. So the virtual joint $v(x)$ is also non-differentiable at ∂x but has essentially the same behaviour like $x \mapsto \max\{0, x\}$ at $x = 0$. Forming the square $x \mapsto (\max\{0, x\})^2$ creates a C^1 function, we will use this trick in our objective function.

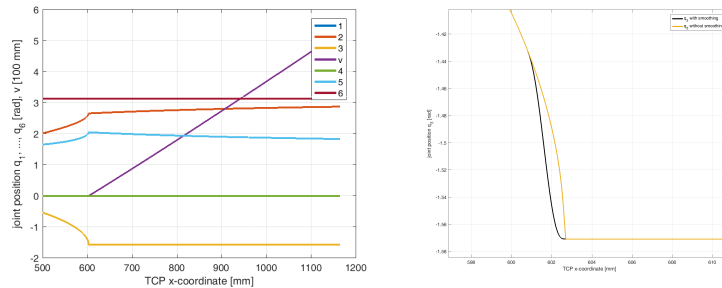


Fig. 4. Joint values for motion through workspace boundary

5 Formulation of the Optimization Problem

We assume that poses must be reached with the same configuration; this is quite usual for Cartesian task. We parametrize the corner frame as $C = \text{Trans}(x, y, z) \cdot R_z(\alpha) \cdot R_y(\beta) \cdot R_x(\gamma)$. These parameters or a subset thereof constitute our optimization variables. Denoting $\tilde{q}^{(k,l)} = \tilde{q}^{(k,l)(C)} = \tilde{q}^{(k,l)}(x, y, z, \alpha, \beta, \gamma)$ the joint

values obtained by the virtual robot backward transform for grid position (k, l) in the box, $q_i^{(k,l)}$ and $v^{(k,l)}$ the original and virtual joints, we may optimize

$$\begin{aligned} \min_{x,y,z,\alpha,\beta,\gamma} & \sum_{k=1}^{B_x} \sum_{l=1}^{B_y} (v^{(k,l)})^2 \\ \text{under} & q_{\min,i} \leq q_i^{(k,l)} \leq q_{\max,i} \\ & i = 1, \dots, 6, k = 1, \dots, B_x, l = 1, \dots, B_y \end{aligned}$$

We can also add constraints on the frame parameters $(x, y, z, \alpha, \beta, \gamma)$. The square in the objective function makes the objective function C^1 . To make advantage of this however we must use the C^2 smoothing of the backward transform at the workspace boundary so that the constraints are C^2 as well. With $|v^{(k,l)}|^3$ we could even obtain a C^3 objective function.

Adding some manipulability criterion from [12] or [8] to the objective function can optimize feasibility and manipulability in combination. However one has to use appropriate weighting because in extreme cases the optimizer might tolerate some infeasible points in exchange for high manipulability at other points.

6 Numerical Results

We have tested our optimization procedure with the solvers implemented in the MATLAB `fmincon` command. We obtained optimal solutions both with the default interior point algorithm and the SQP algorithms. However, in many cases the SQP algorithm required only 10 iterations, about half the iterations of the interior point algorithm. Computation time was below 10 sec on a standard laptop with $B_x \cdot B_y = 5 \cdot 6 = 30$ grid point in the box. Figure 5 shows some typical run where a box is drawn from far outside the workspace (red) to the interior (blue). The results were almost independent from differentiability properties. The interpretation is: Even when crossing the critical workspace boundary the majority of grid points is away from the vertical slope, dominating the numerical derivatives. When sufficiently inside the workspace the algorithm hardly ever enters the infeasible region again.

We have also tested the algorithm with success for a more complicated geometry: The robot makes the moves for the popular board game "Settlers of Catan" with real tokens on a hexagonal structure on a playfield simulated on a screen, see [5]. However some manual intervention is necessary as the robot cannot reach all positions with the same configuration.

7 Conclusions

The approach presented in this contribution opens a way to non-interior-point optimization algorithms for the most common class of industrial 6R robots. Obviously the approach can also be used for the placement of a robot in a fixed

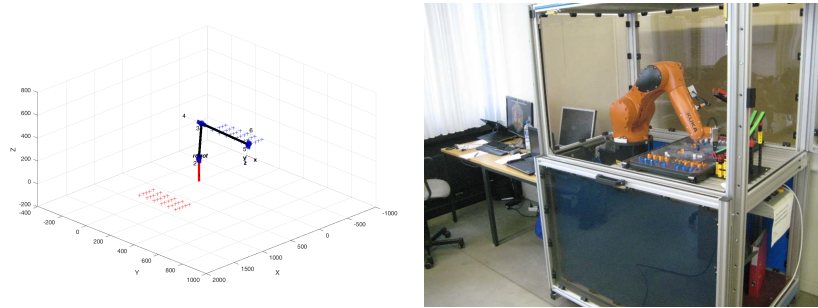


Fig. 5. Optimization results and demonstrator setup

work cell; we only need to consider the robot's base coordinate system as the variable. Furthermore it seems promising to use the idea for the optimization of redundant tasks like in [6] or redundant robots and to compare the results.

New algorithms for non-differentiable problems [3] should be investigated in comparison to higher order approaches, including estimates for the convergence of the solution of the smoothed problem to the original problem's solution.

References

1. Bertsekas, D.P.: Nondifferentiable Optimization via Approximation. *Math. Programming Study* 3, pp. 1-25 (1975).
2. Craig, J.: *Introduction to Robotics: Mechanics and Control*. Addison Wesley, (1986)
3. Curtis, F.E., Overton, M.L.: A Sequential Quadratic Programming Algorithm for Nonconvex, Nonsmooth Constrained Optimization. *SIAM J. Optimization* 22, pp. 474-500 (2012)
4. Garcia, C., Zangwill, W.: *Pathways to solutions, fixed points and equilibria*. Prentice-Hall (1981)
5. KUKA Robot Group: Robots Play Board Games - Students Win Big, https://www.youtube.com/watch?v=oCQPWv_ky2c, (2016)
6. Léger, J., Angeles, J.: Off-line programming of six-axis robots for optimum five-dimensional tasks. *Mechanism and Machine Theory* 100, 155-169 (2016)
7. Leontjevs, V., Flores, F.G., Lopes, J., Kecskemethy, A.: Singularity Avoidance by Virtual Redundant Axis and its Application to Large Base Motion Compensation of Serial Robots In: *Proceedings of the RAAD 2012 21st International Workshop on Robotics in Alpe-Adria-Danube Region*. Naples (2012)
8. Merlet, J.P.: Jacobian, manipulability, condition number, and accuracy of parallel robots. *J. Mech. Des.* 128(1), 199-206 (2006)
9. Nocedal, J., Wright, S.J.: *Numerical Optimization*. Springer, New York (2006)
10. Reiter, A.: Ein Beitrag zur Singularitätsvermeidung bei Industrierobotern durch Einführung virtueller Achsen. Master Thesis, Johannes Kepler University Linz (2015)
11. Vahrenkamp, N., Asfour, T., Dillmann, R.: Robot Placement based on Reachability Inversion. *2013 IEEE International Conference on Robotics and Automation* (2013)
12. Yoshikawa, T.: Manipulability of Robotic Mechanisms *The International Journal of Robotics Research* 4(2), pp. 3-9 (1985).